JOURNAL OF CHEMICAL EDUCATION

pubs.acs.org/jchemeduc

Laboratory Experiment

# Photooxidation of Water with Thin Film Tungsten Oxides

Hal Van Ryswyk,* Aech Loar, Jacob Kelber, Zooey Meznarich, Jocelyn Sabin, Simone Griffith, and Leah E. Stevenson

Cite This: *J. Chem. Educ.* 2021, 98, 614–619

Read Online

ACCESS | Metrics & More | Article Recommendations | Supporting Information

**ABSTRACT:** Tungsten oxide semiconductors are used to photooxidize water. Students prepare $WO_3$, $CuWO_4$, and mixed composition thin film photoanodes. The syntheses are simple, allowing for the quick production of a range of materials. Photoanodes are tested in a photoelectrochemical cell assembled from common equipment, allowing for the direct comparison of photoanode performance. Composite photoanodes perform best, leading to a discussion of what limits overall performance in these materials. Additional instrumental methods such as SEM, EDS, XRD, and diffuse reflectance UV−vis spectrophotometry, if available, can be incorporated readily into the experiment, providing additional insights into material properties. Students are introduced to solid-state chemistry, semiconductors, and the photooxidation of water in the context of the hydrogen economy.

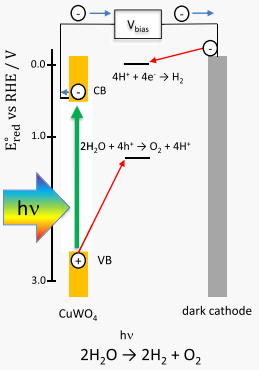


**KEYWORDS:** *Upper-Division Undergraduate, Inorganic Chemistry, Interdisciplinary/Multidisciplinary, Laboratory Instruction, Hands-On Learning/Manipulatives, Electrochemistry, Instrumental Methods, Materials Science, Photochemistry, Semiconductors*



## INTRODUCTION

There is enormous potential for using the energy in sunlight to split water, producing molecular hydrogen fuel.[1] While molecular hydrogen is the high-value product in this scheme, the coevolution of oxygen gas is the more difficult reaction to drive. Photoelectrochemical cells (PECs) use semiconductor electrodes that harvest sunlight and facilitate the splitting of water.[2] The material properties of the electrodes employed in PECs are critical to their function.[3]

Proponents of the hydrogen economy envision hydrogen gas as a low-carbon fuel for heating and transportation, and as a sink for energy storage and long-distance energy transportation. The high gravimetric energy density stored in the hydrogen molecule can be converted directly into electrical energy with high efficiency via a fuel cell. Hydrogen gas is clean burning, producing water as its sole combustion product. Nonetheless, the carbon footprint of the hydrogen economy will be determined by the ultimate source of hydrogen.

Molecular hydrogen does not occur naturally in large reservoirs on Earth. Its manufacture requires a hydrogen source, or carrier, such as a hydrocarbon fossil fuel or water. The majority of hydrogen produced today comes from steam methane re-forming, a process that consumes a hydrocarbon hydrogen carrier and creates carbon monoxide:

$$CH_4(g) + H_2O(g) \rightarrow CO(g) + 3H_2(g) \quad (1)$$

However, the preponderance of hydrogen atoms in the biosphere is carried in water. A process to split water, liberating molecular hydrogen and molecular oxygen and driven by renewable energy, would provide a truly green fuel.

In this context, photoelectrochemistry has been considered a promising approach to split water into hydrogen and oxygen gases.[4] The photoelectrochemical splitting of water can be performed by combining a photoanode with a dark cathode. In general, metal oxide semiconductors are used as photoanodes to evolve oxygen, and metals or photocathodes are used to evolve hydrogen gas. Overall, sunlight powers the carbon-free production of hydrogen gas:

$$2H_2O(l) \xrightarrow{h\nu} 2H_2(g) + O_2(g) \quad (2)$$

Fujishima and Honda[5] were photoelectrochemical pioneers in the early 1970s, using wide band gap, n-type $TiO_2$ to split water, while Hodes et al.[6] introduced $WO_3$ a few years later. This *Journal* documented the early advances in PECs for the direct conversion of sunlight into chemical fuels such as hydrogen,[7−9] while recent reports address the electrochemistry of semiconductor-assisted photooxidation[10,11] and the catalysis of water photooxidation.[12−16] All of this work is grounded in a firm understanding of electrocatalysis in water splitting,[17] the

**Received:** July 20, 2020
**Revised:** November 30, 2020
**Published:** December 23, 2020

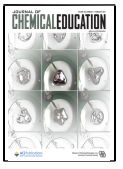

insights provided by electrochemical techniques,[18] the energetics of photochemical reactions,[19] and an understanding of photo quantum yield.[20]

Semiconductors suitable as electrodes for the photoelectrolysis of water with sunlight require the following:[21]

(i) moderate conductivity (preferably due to a combination of large carrier mobility and small carrier concentration);
(ii) a minimal number of recombination centers;
(iii) chemical stability both in the dark and under illumination;
(iv) a band gap of approximately 1.8−2.1 eV to maximize solar radiation absorption and drive the reaction at a rate sufficient for practical fuel production; and
(v) to a first approximation, suitable positioning of the conduction and valence band edges relative to the $H^+/H_2$ and $O_2/H_2O$ reduction potentials, respectively.

While these requirements have been understood for almost 50 years, there is no ideal candidate meeting all of these criteria. Of known compounds, metal oxides show promise in a number of these areas and have been studied extensively. Many such as $TiO_2$ have the required long-term stability for practical use.[22] Some such as $\alpha$-$Fe_2O_3$ have band gaps that extend into the visible.[23] $WO_3$ and $CuWO_4$ are metal oxide semiconductors of moderate conductivity with few recombination centers and good-to-excellent chemical stability.[24] The fifth condition speaks to the spontaneity of the water splitting reaction for a PEC wherein the semiconductor electrode is equilibrated directly with the hydrogen and oxygen evolution reactions. This condition is not absolute, and in cases where the band alignment is not ideal, it is still possible to split water with the addition of a small amount of electrical energy to supplement the energy derived from sunlight. A few metal oxide semiconductors remain good candidates for use as photoanodes in light-assisted water splitting in this limit.

The band diagrams for $WO_3$ and $CuWO_4$, wide band gap n-type semiconductors, are shown in Figure 1. The band gap,

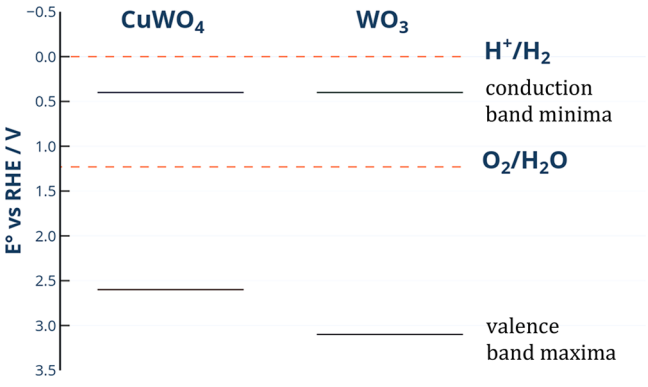


**Figure 1.** Band diagrams for $WO_3$ and $CuWO_4$ showing the standard reduction potentials for $H^+$ and $O_2$. The positions of the $WO_3$ and $CuWO_4$ band edges are taken from the literature.[27,29]

equal to the difference between the conduction and valence band edges, is typically determined from optical measurements, and the position of the conduction band edge is determined from electrochemical impedance spectroscopy.[25] Their conduction bands, largely of W(5d) character, are at the same potential,[26,27] slightly more positive than the standard reduction potential of protons. The valence bands, with O(2p) and Cu(3d) + O(2p) character, respectively, have edges significantly positive of the standard reduction potential of oxygen, $E^\circ$ = +1.23 V vs NHE at pH = 0. The 2.7 eV band gap of $WO_3$ is on the edge of the visible, whereas $CuWO_4$ with a smaller band gap of 2.2 eV will absorb more solar radiation. $WO_3$ is stable in solutions having a pH below 7, whereas the chemical stability of $CuWO_4$ at moderate to high pH is superior.[27,28]

Figure 2 shows $CuWO_4$ in a PEC photooxidizing water with the addition of a low applied potential to enable the reduction

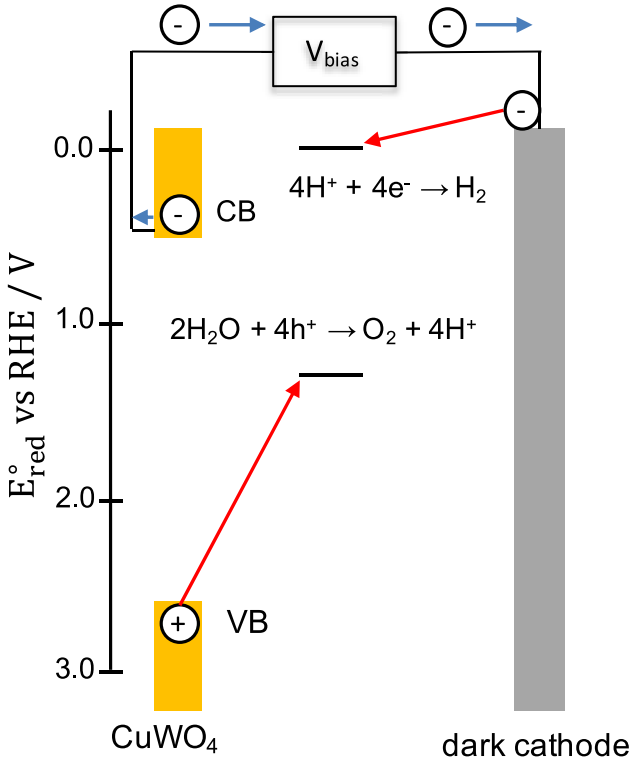


**Figure 2.** Energy diagram for a PEC with a $CuWO_4$ photoanode and a dark cathode. A photon with energy greater than the band gap of $CuWO_4$ has been absorbed by the photoanode, producing the electron/hole pair at the edges of the conduction (CB) and valence bands (VB). The transport of electrons is shown with blue arrows while interfacial electrochemistry due to electron or hole transfer is shown in red. The hole oxidizes water at the photoanode while the electron is transferred via the circuit to the dark cathode, where, with the addition of a small amount of electrical energy, the electron reduces protons.

of protons at the dark cathode. The $CuWO_4$ photoanode absorbs light, promoting an electron from the valence band to the conduction band and leaving a hole in the valence band. Given the position of the valence band edge relative to the reduction potential of oxygen, holes ($h^+$) in the valence band are sufficiently energetic such that they can react with water to produce oxygen gas:

$$2H_2O + 4h^+ \rightarrow O_2(g) + 4H^+ \quad (3)$$

However, an electron at the conduction band edge is not sufficiently energetic to react with protons in water to produce hydrogen gas:

$$4H^+ + 4e^- \rightarrow 2H_2(g) \quad (4)$$

Nevertheless, the electron can be transferred via the external contact of the photoanode to the dark cathode, and the


https://dx.doi.org/10.1021/acs.jchemed.0c00976
J. Chem. Educ. 2021, 98, 614−619

potential of the electron can made more negative than the reduction potential for protons with a small input of electrical energy, allowing reaction 4 to proceed. In terms of the overall energetics, the majority of the energy for splitting water is supplied by the photon.

Practical metal oxide photoanodes are fabricated as thin films. Keeping the film thickness smaller than the hole diffusion length allows photogenerated carriers throughout the semiconductor to move to the surface where they are harvested without excessive loss. Utilizing thin films also minimizes the total amount of material required when constructing large area devices. While $WO_3$ was typically formed through the anodization of tungsten metal,[6] thin films of both $WO_3$ and $CuWO_4$ can be produced easily via electrodeposition,[27,28,30] spin coating,[31] or drop-casting[32] from W(VI) precursors prior to calcination in air at moderate temperatures.

While a deep exploration of the five criteria for effective photoelectrolysis listed above is not possible in the course of a single experiment, the interplay of absorbance, electron−hole recombination, and electrocatalysis across $WO_3$, $CuWO_4$, and a range of their composites can be examined in PEC test cells, yielding insights into the material properties required for the effective splitting of water with sunlight.

## EXPERIMENTAL OVERVIEW

The production of photoanodes with varying compositions, followed by characterization in a PEC, is at the core of this experiment. Detailed procedures for the production and characterization of photoanodes are provided in the Supporting Information along with a list of required equipment and chemicals. The only required, nonroutine equipment is a programmable furnace capable of reaching 550 °C and a potentiostat.

Thin films of $WO_3$, $CuWO_4$, and mixed composition $CuWO_4/WO_3$ semiconductors are prepared in parallel by drop-casting solutions of ammonium metatungstate hydrate and copper nitrate trihydrate salts in ethylene glycol solution onto fluorine-doped tin oxide (FTO) substrates.[32] The substrates are dried at 120 °C in air for 30 min and then transferred to a programmable furnace for calcination at 550 °C in air.

A PEC test rig is assembled from

- a potentiostat;
- a reference electrode;
- a carbon rod;
- a suitable optical source;
- a 150 mL beaker;
- a lab jack; and
- a ring stand with associated clamps.

Linear scan voltammetry (LSV) is used to collect current−voltage curves under simulated solar irradiation and in the dark. While the data presented here were acquired with an AM1.5G source that reproduces solar irradiance, a ceramic metal halide grow light is a highly effective, readily available, low-cost substitute. Alternately, either a bright metal halide desk lamp or a slide projector is a source sufficient to accomplish the goals of the experiment.

### Extensions

The photoanodes are readily amenable to characterization by a number of instrumental techniques. Energy dispersive X-ray spectroscopy (EDS) probes elemental composition and is particularly useful when working with composite samples. X-ray diffraction (XRD) provides information on crystal structure, unit cell dimensions, and crystallite size. Secondary electron scanning electron microscopy (SEM) details the surface morphology including the dimensions of mesopores. Diffuse reflectance UV−vis spectrophotometry addresses the interaction of the nanostructured thin films with visible light.

In addition, an electrocatalyst for the oxygen evolution reaction (OER) greatly enhances performance. A manganese phosphate electrocatalyst incorporated onto the surface of the photoanode can increase the overall rate of oxygen evolution by up to 50%.[32]

### Logistics

The experiment, typically run with students working in pairs, has been offered five times in an upper-division instrumental methods laboratory, in an upper-division materials chemistry hybrid laboratory/tutorial, and in a first-year introduction to chemical research laboratory. One 4 h laboratory session is dedicated to production of the photoanodes, with 2 h on a subsequent day set aside for PEC characterization. An additional 2 h session allows for roughly six samples to be characterized by SEM and EDS, while four samples can be characterized by high-resolution XRD at the same time.

## HAZARDS

Cutting glass often produces small glass shards. Wear gloves when handling sheets of substrates and cutting glass. Sweep the working area benchtop immediately after cutting glass. AM1.5G and grow light sources emit ultraviolet light. Use appropriate shielding, and minimize exposure of eyes and skin.

## RESULTS AND DISCUSSION

Figure 3 shows current−voltage curves for the two homogeneous semiconductor photoanodes and a composite photoanode of 1:4 $CuWO_4$:$WO_3$. Positive current represents oxidation at the photoanode. Light from the optical source is alternately allowed to illuminate the cell or is blocked via insertion of a cardboard shutter by hand at roughly 0.2 Hz to provide an internal, dark current baseline for each run. Negligible current flows in the dark for all three materials, while under illumination considerable current is seen starting at potentials well negative of $E_{O_2}$, which is +0.738 V vs Ag/AgCl/sat. KCl in the 0.1 M $Na_2SO_4$ electrolyte at pH 5. The photocurrent to oxygen conversion efficiency at $WO_3$ in this electrolyte exceeds 88%;[28] thus, photocurrent is a convenient measure of oxygen gas production.

All three materials photooxidize water at $E_{O_2}$. The application of increasingly positive potential produces even more oxygen as the activation barrier for the OER is surmounted in this system that is not mass transport limited. Most importantly, oxygen produced under illumination at potentials well *negative* of $E_{O_2}$ is clear evidence of solar light-to-chemical energy conversion for all three materials; the energy of photons is harvested to drive the OER at applied potentials where it would not occur at a dark electrode.

Oxygen production for a photoanode is a function of absorbance, carrier separation and transport, and electrochemical kinetics at the semiconductor/solution interface. The energy of light absorbed by a material is governed by its band gap, which describes how far into the spectrum of visible light the material will harvest photons. The amount of light absorbed is governed by the material's absorption coefficient,


https://dx.doi.org/10.1021/acs.jchemed.0c00976
J. Chem. Educ. 2021, 98, 614−619

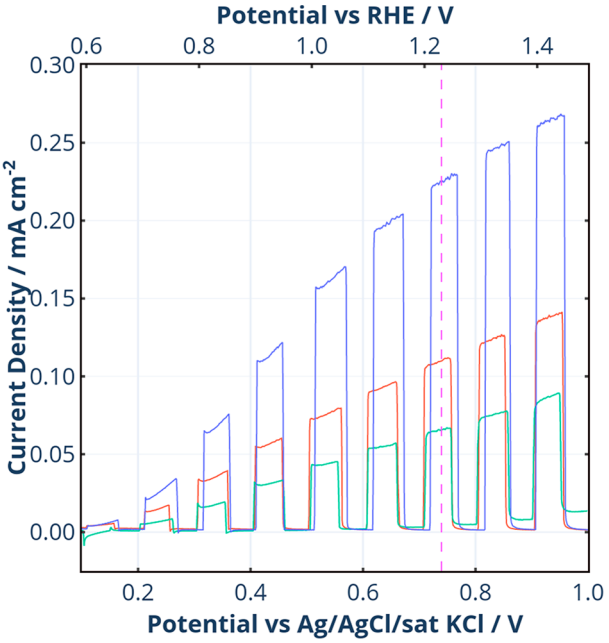


**Figure 3.** Linear scan voltammograms for photoanodes composed of $WO_3$ (red), $CuWO_4$ (green), and 1:4 $CuWO_4$:$WO_3$ (blue) in 0.1 M $Na_2SO_4$ at pH 5 illuminated with an AM1.5G source at 100 mW $cm^{-2}$. The scan is initiated at +0.1 V vs Ag/AgCl/sat. KCl at a rate of 25 mV $s^{-1}$, and the source intensity is chopped by hand at roughly 0.2 Hz. The dashed line marks $E_{O_2}$.

which describes how many photons are absorbed per unit thickness, and the material's surface morphology, which influences how much light is scattered rather than absorbed. Once a photon has been absorbed and an electron/hole pair created, these charged carriers must be separated, with the hole moving to the semiconductor/solution interface and the electron to the back of the electrode where it is shuttled into the external circuit and transferred to the dark cathode. If the electron/hole pair is allowed to recombine, then the electrochemical water splitting reaction will not be achieved and the energy of the absorbed photon will be converted to heat. Last, once the hole is delivered to the semiconductor/solution interface, the electrochemical kinetics of the OER determine the amount of oxygen produced.

The figure of merit for photoanode performance is the current density at $E_{O_2}$ under illumination. As shown in Table 1,

**Table 1. Thin Film Photoanode Average Current Densities at $E_{O_2}$ under AM1.5G Illumination**

| composition | $j$/(mA $cm^{-2}$)[a] |
|---|---|
| $WO_3$ | 0.105 ± 0.004 |
| $CuWO_4$ | 0.058 ± 0.006 |
| 1:4 $CuWO_4$:$WO_3$ | 0.232 ± 0.016 |

[a]Standard deviation values for $n$ = 3.

$WO_3$ performs slightly better than $CuWO_4$ for the drop-cast electrodes produced here. Considering only absorbance, this is counterintuitive, given that $CuWO_4$ with its smaller band gap should utilize more of the solar irradiance with its onset of absorbance at 540 nm vs 460 nm for $WO_3$. When seeking an absorbance-based explanation, the relative behavior of the pair could be due to differences in crystallite size (instructor notes, Figure S6), with greater light scattering occurring at the more highly textured $CuWO_4$ decreasing the number of photons absorbed. With the consideration of carrier separation and transport, superior $WO_3$ photocurrents could be explained by the drop-cast $CuWO_4$ having lower carrier mobility and greater recombination, in effect giving up a greater fraction of carriers than $WO_3$. In terms of overall performance of pure, thin film photoanodes, the relative photocurrents observed here are consistent with reports of drop-cast $WO_3$ and $CuWO_4$ showing roughly identical photooxidation current densities.[32]

Composite photoanodes produce considerably more photooxidation than their pure constituents. The absorbance and electrochemical kinetics of the individual constituents are unlikely to change when the materials are combined in the composite. Thus, the improved performance of composites is likely due to enhancements in carrier separation and transport therein. Nam et al. propose a two-step mechanism to explain this behavior.[32] In the first step, holes formed in the valence band of $WO_3$ transfer to the valence band of $CuWO_4$, while in the second step electrons in the conduction band of $CuWO_4$ transfer to the conduction band of $WO_3$. The driving force for the first step is readily apparent in Figure 1: holes formed in the $WO_3$ valence band can "bubble upwards" roughly 0.5 eV by moving from $WO_3$ to $CuWO_4$. While there is no net driving force for the second step, it is akin to a sensitization of the larger band gap semiconductor by the smaller, wherein electrons from the $CuWO_4$ are injected into the $WO_3$. The net result is a segregation of carriers in adjacent materials, leading to decreased recombination. An alternate mechanism consistent with the data involves enhanced carrier transport wherein interfacial defect centers at grain boundaries in the composite materials are healed by the second material present, producing longer carrier diffusion lengths and less recombination.

Finally, with regard to electrochemical kinetics, the limiting reaction in the PEC is the OER. When paired with the hydrogen evolution reaction (HER) at the dark cathode, water is electrolyzed with a photoassist. Of the two reactions, the OER is the more difficult to accomplish. This experiment focuses on driving the OER with a photoassist. While the surfaces of the photoanodes produced here have some photocatalytic capacity, the addition of an electrocatalyst, $Mn_5(PO_3(OH))_2(PO_4)_2(H_2O)_4$, greatly enhances the OER. (See the extensions in the instructor notes.) In this fashion, the material properties of the photoanode suitable for the photooxidation of water can be addressed separately.

## Extensions

Additional instrumental techniques, if available, greatly aid in the characterization of the photoanodes. EDS of $WO_3$ photoanodes shows signals from only W and O, with Sn from the FTO substrate also present (Figure S7). $CuWO_4$ shows equal atomic percentages of Cu and W (Figure S8), while the ratio of Cu:W is 1:4 in a mixed composition photoanode produced from a 1:4 ratio of metals in the drop-casting solution (Figure S9).

XRD shows that the $WO_3$ produced after calcination at 550 °C is monoclinic,[33] whereas the $CuWO_4$ is triclinic[29] (Figure S5). Composite photoanodes show both $WO_3$ and $CuWO_4$ features. The lines observed can be indexed from calculated crystal structures, either directly via databases such as The Materials Project,[34,35] or with software such as VESTA[36] or CrystalMaker[37] to visualize the unit cell from experimental


https://dx.doi.org/10.1021/acs.jchemed.0c00976
J. Chem. Educ. 2021, 98, 614−619

data in The American Mineralogist Crystal Structure Database,[38] and VESTA or CrystalDiffract[37] subsequently to calculate powder patterns.

SEM shows that $WO_3$ thin films form a smooth surface of 20−50 nm crystallites, whereas the $CuWO_4$ forms an open porous system of 10−20 nm diameter crystallites. Composite films show congealed $WO_3$ islands in a porous sea of smaller $CuWO_4$ crystallites (Figure S6).

Diffuse reflectance UV−vis spectrophotometric data correlates nicely with band gaps and the observed colors (Figure S10).

## STUDENT LEARNING

This experiment focuses on understanding the effects of band gap, charge separation and transport, and interfacial electron transfer kinetics of the OER on the ability of metal oxide photoanodes to split water using evidence from a PEC and various instrumental techniques. Learning objectives were assessed via a rubric applied to final reports and posters. Students demonstrated a strong understanding of and the ability to explain the effects of band gap and charge separation and transport upon the production of oxygen at a photoanode under illumination using data collected from electrochemical techniques. Their understanding of the role of interfacial electron transfer kinetics for the OER on the production of oxygen was weak in the first offering of this experiment. Subsequent revisions in the introductory materials, as well as the addition of an informal white board talk on this subject during down time on the first day of the experiment, greatly enhanced student learning on this point. Finally, students were able to integrate data from multiple instrumental techniques to support their arguments.

Students self-identified challenges in recalling and applying concepts of cell potentials. Students were almost uniformly appreciative of the ability to synthesize a material that could split water with sunlight, and many found the opportunity to apply multiple techniques to a solid-state system to form a more complete, unifying picture gratifying.

## SUMMARY

Thin film photoanodes of $WO_3$ and $CuWO_4$ can be easily fabricated in a short time and their performance in the photooxidation of water measured with a simple photoelectrochemical cell. While additional instrumental techniques lend insights into material properties, the core content of this experiment allows students an opportunity to observe how semiconductor properties affect the performance of a photoanode in a key reaction at the heart of the hydrogen economy.

## ASSOCIATED CONTENT

### Supporting Information

The Supporting Information is available at https://pubs.acs.org/doi/10.1021/acs.jchemed.0c00976.

Experimental protocol including introduction and student directions (PDF, DOCX)

Notes for instructors (PDF, DOCX)

## AUTHOR INFORMATION


### Corresponding Author

**Hal Van Ryswyk** − *Department of Chemistry, Harvey Mudd College, Claremont, California 91711, United States;* orcid.org/0000-0002-1701-6194; Email: vanryswyk@hmc.edu

### Authors

**Aech Loar** − *Department of Chemistry, Harvey Mudd College, Claremont, California 91711, United States*

**Jacob Kelber** − *Department of Chemistry, Harvey Mudd College, Claremont, California 91711, United States*

**Zooey Meznarich** − *Department of Chemistry, Harvey Mudd College, Claremont, California 91711, United States*

**Jocelyn Sabin** − *Department of Chemistry, Harvey Mudd College, Claremont, California 91711, United States*

**Simone Griffith** − *Department of Chemistry, Harvey Mudd College, Claremont, California 91711, United States*

**Leah E. Stevenson** − *Department of Chemistry, Harvey Mudd College, Claremont, California 91711, United States*

Complete contact information is available at: https://pubs.acs.org/10.1021/acs.jchemed.0c00976


### Notes

The authors declare no competing financial interest.

## ACKNOWLEDGMENTS

The authors thank Adam R. Johnson for helpful discussions. The National Science Foundation supported acquisition of the scanning electron microscope through DMR-1126080.

## REFERENCES


(1) Kim, J. H.; Hansora, D.; Sharma, P.; Jang, J.-W.; Lee, J. S. Toward Practical Solar Hydrogen Production − an Artificial Photosynthetic Leaf-to-Farm Challenge. *Chem. Soc. Rev.* **2019**, *48* (7), 1908−1971.

(2) Walter, M. G.; Warren, E. L.; McKone, J. R.; Boettcher, S. W.; Mi, Q.; Santori, E. A.; Lewis, N. S. Solar Water Splitting Cells. *Chem. Rev.* **2010**, *110* (11), 6446−6473.

(3) Saraswat, S. K.; Rodene, D. D.; Gupta, R. B. Recent Advancements in Semiconductor Materials for Photoelectrochemical Water Splitting for Hydrogen Production Using Visible Light. *Renewable Sustainable Energy Rev.* **2018**, *89*, 228−248.

(4) Finklea, H. O. Photoelectrochemistry: Introductory Concepts. *J. Chem. Educ.* **1983**, *60* (4), 325.

(5) Fujishima, A.; Honda, K. Electrochemical Photolysis of Water at a Semiconductor Electrode. *Nature* **1972**, *238* (5358), 37−38.

(6) Hodes, G.; Cahen, D.; Manassen, J. Tungsten Trioxide as a Photoanode for a Photoelectrochemical Cell (PEC). *Nature* **1976**, *260* (5549), 312−313.

(7) Wrighton, M. S. Photoelectrochemistry: Inorganic Photochemistry at Semiconductor Electrodes. *J. Chem. Educ.* **1983**, *60* (10), 877−881.

(8) Wrighton, M. S. Chemically Derivatized Semiconductor Photoelectrodes. *J. Chem. Educ.* **1983**, *60* (4), 335−337.

(9) Parkinson, B. An Overview of the Progress in Photoelectrochemical Energy Conversion. *J. Chem. Educ.* **1983**, *60* (4), 338−340.

(10) Spitler, M. T. Dye Photooxidation of Semiconductor Electrodes: A Corollary to Spectral Sensitization in Photography. *J. Chem. Educ.* **1983**, *60* (4), 330−332.

(11) Rajeshwar, K.; Ibanez, J. G. Electrochemical Aspects of Photocatalysis: Application to Detoxification and Disinfection Scenarios. *J. Chem. Educ.* **1995**, *72* (11), 1044−1049.

(12) Shaner, S. E.; Hooker, P. D.; Nickel, A.-M.; Leichtfuss, A. R.; Adams, C. S.; de la Cerda, D.; She, Y.; Gerken, J. B.; Pokhrel, R.; Ambrose, N. J.; Khaliqi, D.; Stahl, S. S.; Schuttlefield Christus, J. D. Discovering Inexpensive, Effective Catalysts for Solar Energy

Conversion: An Authentic Research Laboratory Experience. *J. Chem. Educ.* **2016**, *93* (4), 650−657.
(13) Anunson, P. N.; Winkler, G. R.; Winkler, J. R.; Parkinson, B. A.; Schuttlefield Christus, J. D. Involving Students in a Collaborative Project To Help Discover Inexpensive, Stable Materials for Solar Photoelectrolysis. *J. Chem. Educ.* **2013**, *90* (10), 1333−1340.
(14) Zhang, R.; Liu, S.; Yuan, H.; Xiao, D.; Choi, M. M. F. Nanosized $TiO_2$ for Photocatalytic Water Splitting Studied by Oxygen Sensor and Data Logger. *J. Chem. Educ.* **2012**, *89* (10), 1319−1322.
(15) Li, X.; Deng, Y.; Jiang, Z.; Shen, R.; Xie, J.; Liu, W.; Chen, X. Photocatalytic Hydrogen Production over CdS Nanomaterials: An Interdisciplinary Experiment for Introducing Undergraduate Students to Photocatalysis and Analytical Chemistry. *J. Chem. Educ.* **2019**, *96* (6), 1224−1229.
(16) Ma, J.; Guo, R. Engaging in Curriculum Reform of Chinese Chemistry Graduate Education: An Example from a Photocatalysis—Principles and Applications Course. *J. Chem. Educ.* **2014**, *91* (2), 206−210.
(17) Gonçalves, R. H. Reusing a Hard Drive Platter To Demonstrate Electrocatalysts for Hydrogen and Oxygen Evolution Reactions. *J. Chem. Educ.* **2018**, *95* (2), 290−294.
(18) Hendel, S. J.; Young, E. R. Introduction to Electrochemistry and the Use of Electrochemistry to Synthesize and Evaluate Catalysts for Water Oxidation and Reduction. *J. Chem. Educ.* **2016**, *93* (11), 1951−1956.
(19) Kutal, C. Photochemical Conversion and Storage of Solar Energy. *J. Chem. Educ.* **1983**, *60* (10), 882−887.
(20) Barcelò, A. R.; Zapata, J. M. Measurement of Quantum Yield, Quantum Requirement, and Energetic Efficiency of the $O_2$-Evolving System of Photosynthesis by a Simple Dye Reaction. *J. Chem. Educ.* **1996**, *73* (11), 1034−1035.
(21) Grimes, C.; Varghese, O.; Ranjan, S. Photoelectrolysis. In *Light, Water, Hydrogen: The Solar Generation of Hydrogen by Water Electrolysis*; Springer: Boston, 2008.
(22) Li, R.; Weng, Y.; Zhou, X.; Wang, X.; Mi, Y.; Chong, R.; Han, H.; Li, C. Achieving Overall Water Splitting Using Titanium Dioxide-Based Photocatalysts of Different Phases. *Energy Environ. Sci.* **2015**, *8* (8), 2377−2382.
(23) Sharma, P.; Jang, J.; Lee, J. S. Key Strategies to Advance the Photoelectrochemical Water Splitting Performance of $\alpha$-$Fe_2O_3$ Photoanode. *ChemCatChem* **2019**, *11* (1), 157−179.
(24) Yourey, J. E.; Pyper, K. J.; Kurtz, J. B.; Bartlett, B. M. Chemical Stability of $CuWO_4$ for Photoelectrochemical Water Oxidation. *J. Phys. Chem. C* **2013**, *117* (17), 8708−8718.
(25) Beranek, R. (Photo)Electrochemical Methods for the Determination of the Band Edge Positions of $TiO_2$-Based Nanomaterials. *Adv. Phys. Chem.* **2011**, *2011*, 1−20.
(26) Desilvestro, J.; Grätzel, M. Photoelectrochemistry of Polycrystalline n-$WO_3$: Electrochemical Characterization and Photoassisted Oxidation Processes. *J. Electroanal. Chem. Interfacial Electrochem.* **1987**, *238* (1), 129−150.
(27) Yourey, J. E.; Bartlett, B. M. Electrochemical Deposition and Photoelectrochemistry of CuWO4, a Promising Photoanode for Water Oxidation. *J. Mater. Chem.* **2011**, *21* (21), 7651−7660.
(28) Hill, J. C.; Choi, K.-S. Effect of Electrolytes on the Selectivity and Stability of n-Type $WO_3$ Photoelectrodes for Use in Solar Water Oxidation. *J. Phys. Chem. C* **2012**, *116* (14), 7612−7620.
(29) Gaillard, N.; Chang, Y.; DeAngelis, A.; Higgins, S.; Braun, A. A Nanocomposite Photoelectrode Made of 2.2 eV Band Gap Copper Tungstate $CuWO_4$ and Multi-Wall Carbon Nanotubes for Solar-Assisted Water Splitting. *Int. J. Hydrogen Energy* **2013**, *38* (8), 3166−3176.
(30) Baeck, S.-H.; Choi, K.-S.; Jaramillo, T. F.; Stucky, G. D.; McFarland, E. W. Enhancement of Photocatalytic and Electrochromic Properties of Electrochemically Fabricated Mesoporous $WO_3$ Thin Films. *Adv. Mater.* **2003**, *15* (15), 1269−1273.
(31) Pyper, K. J.; Yourey, J. E.; Bartlett, B. M. Reactivity of $CuWO_4$ in Photoelectrochemical Water Oxidation is Dictated by a Midgap Electronic State. *J. Phys. Chem. C* **2013**, *117* (47), 24726−24732.
(32) Nam, K. M.; Cheon, E. A.; Shin, W. J.; Bard, A. J. Improved Photoelectrochemical Water Oxidation by the $WO_3$/$CuWO_4$ Composite with a Manganese Phosphate Electrocatalyst. *Langmuir* **2015**, *31* (39), 10897−10903.
(33) Pokhrel, S.; Birkenstock, J.; Dianat, A.; Zimmermann, J.; Schowalter, M.; Rosenauer, A.; Ciacchi, L. C.; Mädler, L. In Situ High Temperature X-Ray Diffraction, Transmission Electron Microscopy and Theoretical Modeling for the Formation of $WO_3$ Crystallites. *CrystEngComm* **2015**, *17* (36), 6985−6998.
(34) Persson, K. The Materials Project: $WO_3$. https://next-gen.materialsproject.org/materials/mp-19033/ (accessed 2020-12-21).
(35) Persson, K. The Materials Project: $CuWO_4$. https://next-gen.materialsproject.org/materials/mp-22773/ (accessed 2020-12-21).
(36) Momma, K.; Izumi, F. VESTA—Visualization for Electronic and STructrual Analysis. https://jp-minerals.org/vesta/en/ (accessed 2020-11-30).
(37) CrystalMaker. http://crystalmaker.com (accessed 2020-11-30).
(38) Downs, R. T.; Hall-Wallace, M. The American Mineralogist Crystal Structure Database. *Am. Mineral.* **2003**, *88*, 247−250. http://www.minsocam.org/MSA/Crystal_Database.html


https://dx.doi.org/10.1021/acs.jchemed.0c00976
*J. Chem. Educ.* 2021, 98, 614−619